Proc. Indian Acad. Sci. (Math. Sci.) Vol. 119, No. 5, November 2009, pp. 679–698.

A further note on the force discrepancy for wing theory in Euler flow

EDMUND CHADWICK and ALI HATAM

School of Computing, Science and Engineering, University of Salford, Salford, M5 4WT, UK
E-mail: e.a.chadwick@salford.ac.uk

MS received 16 October 2008; revised 11 June 2009

Abstract. Uniform steady potential flow past a wing aligned at a small angle to the flow direction is considered. The standard approach is to model this by a vortex sheet, approximated by a finite distribution of horseshoe vortices. In the limit as the span of the horseshoe vortices tends to zero, an integral distribution of infinitesimal horseshoe vortices over the vortex sheet is obtained. The contribution to the force on the wing due to the presence of one of the infinitesimal horseshoe vortices in the distribution is focused upon. Most of the algebra in the force calculation is evaluated using Maple software and is given in the appendices. As in the two previous papers by the authors on wing theory in Euler flow [E Chadwick, A slender-wing theory in potential flow, *Proc. R. Soc.* **A461** (2005) 415–432, and E Chadwick and A Hatam, The physical interpretation of the lift discrepancy in Lanchester–Prandtl lifting wing theory for Euler flow, leading to the proposal of an alternative model in Oseen flow, *Proc. R. Soc.* **A463** (2007) 2257–2275], it is shown that the normal force is half that expected. In this further note, in addition it is demonstrated that the axial force is infinite. The implications and reasons for these results are discussed.

Keywords. Potential flow; Oseen flow; asymptotics.

1. Introduction

It is over 250 years since Euler presented the Euler equations for fluid flow [11], and they have proven extraordinarily successful in describing a wide range of flow fields [20] which would have otherwise been intractable if the viscous Navier–Stokes equations had been used. The Euler equations use the assumption that the fluid does not impart any resistance to motion, and so the viscosity is set to zero. Unfortunately, this manifests in some artificial results, the most well-known being D'Alembert's paradox [4], that the drag force on a closed body encompassed by closed streamlines is zero.

Less well-known, there have been theoretical concerns regarding Euler flow models raised by Goldstein (p. 131–134 of [13]) who questions their validity. He argues that there is more than one limit for the Navier–Stokes equations at high Reynolds number, and the limit producing the Euler equations is not the appropriate one for real flows. He explains that in a real flow, viscous diffusion takes place to remove any discontinuities or singularities present in the flow field. In a real flow, viscous terms should be retained within the limiting procedure. Similarly, Batchelor [3] states that the appropriate approximation to be made for the far-field line vortex is such that it retains the viscous terms within an Oseen flow field.

The line vortex in Oseen flow is given by Chadwick [10]. Fukumoto and Moffatt [12] give the same argument to find the appropriate velocity terms near a vortex ring. By including viscosity, the kinetic energy associated with these flow fields is now bounded, rather than unbounded in the purely inviscid models (see Appendix A).

In the far-field, the Oseen equations hold and these viscous terms can be found. Chadwick [7] gives a far-field expansion for the Oseen velocity and demonstrates that in general the velocity decomposition into an inviscid part and a viscous part, the Lamb-Goldstein velocity decomposition, does not hold, and instead inviscid and viscous terms are coupled together. This is also found by Venkatalaxmi *et al* [24] who demonstrated that the Lamb-Goldstein velocity decompostion does not produce a general solution, and propose a general solution such that the viscous and potential velocity parts are coupled in a similar way as given by the expressions for the oseenlets [19]. The coupled viscous terms provide a significant lift contribution as demonstrated in the case of lift on a slender body [8] and on a wing [9]. The coupled viscous and inviscid terms contribute equally to the lift regardless of the Reynolds number [9]. By contrast, in the inviscid Euler models viscosity is set to zero. The physical interpretation of the omission of viscosity has been identified [6] as the existence of unnatural singularies in the pressure field across the trailing vortex sheet at the trailing edge. The presence of these singularities in the Euler representation is fortuitously ignored in the lift calculation for Euler flows, giving a fortuitous agreement with the real flow [9, 6].

In this paper, this discrepancy in the Euler representation is investigated further by evaluating the axial force and side force as well as the normal force for a uniform flow field at a slight angle of attack given by the inviscid Euler representation. Hence, the coupled viscous contributions which remove the unnatural flow singularites are not considered, which consequently produces some unphysical results. However, the force calculations for this problem require detailed and involved integrals. So these are evaluated by using Maple [2] and for brevity the results of these tedious calculations are presented in various appendices. The normal force agrees with and confirms the previous unphysical result obtained by Chadwick in [9, 6], and in addition the axial force is demonstrated to be infinite due to calculations arising from the singular pressure field. This clearly demonstrates that the forces generated in the inviscid Euler model are unphysical, and this is a consequence of the singular pressure field which is also unphysical. This result is not altogether surprising because it is easily verified that the kinetic energy associated with the fluid in the Euler model is also infinite (see appendix A). Once the flow is regularized (the singularities removed) by the inclusion of viscosity, this artificial discrepancy arising in the Euler model disappears.

For potential and incompressible flow problems, the velocity potential satisfies the Laplace equation, and the Euler equations reduce to the Bernouilli equation. In the standard aerodynamic theory for flow past wings, a further assumption is made by supposing a discontinuous trailing vortex sheet emanating from the trailing edge and is transported downstream such that at the trailing edge the Kutta condition holds, and on the body surface the impermeability condition holds. The Kutta condition [15] states that the flow departs from the trailing edge smoothly. The impermeability condition states that the fluid does not flow into the body and so must be tangential to its surface. This is satisfied to first order by the vortex sheet representation, in the Lanchester–Prandtl model for wing theory [14]. Numerical schemes such as the vortex-lattice method discretize the vortex sheet by replacing it with a finite summation of horseshoe vortices (§11 of [18], §7.8 of [4, 14]). The horseshoe vortex consists of two trailing line vortices which are transported

downstream in the wake, connected by a span-wise line vortex positioned within or on the wing surface. The total lift is obtained by summing all the contributions of lift from the individual horseshoe vortices. In the limit as the spacing between the horseshoe vortices is reduced and tends to zero, the representation of the vortex sheet by an integral distribution of infinitesimal horseshoe vortices is recovered (§8.5 of [23]). In many codes which aim to calculate the lift force, the trailing vortex sheet is assumed to lie on a flat plane whose direction is governed by the direction of the trailing edge. In the present paper, we do the same and consider a steady inviscid vortex sheet which is flat and straight. It is noted though that for a real flow this steady solution is unstable and roll-up occurs at the spanwise ends, and also the sheet curves towards the uniform flow direction in the far-field wake due to viscous forces. However, in the present paper the aim is to determine the body forces in the Euler flow model. The generally accepted force evaluation from such Euler models has proved highly accurate and the numerical code itself stable, and these codes are used extensively by the aerodynamics industry. However, these force evaluations do not consider contributions from across the trailing edge which cut across the trailing vortex sheet and are non-zero because the pressure is singular. As in the papers [9, 6], these evaluations are found in the present paper by considering a single lifting element which is equivalent to an infinitesimal horseshoe vortex. At infinity, the trailing wake looks to first order like an infinitesimal horseshoe vortex, and lower order terms do not contribute to the forces. Therefore, although the force integrals themselves are complex and non-linear, focusing on a single lifting element rather than a distribution of elements is justified. (A distribution of these elements models the vortex sheet, whose strength in turn is determined by applying the impermeability and Kutta condition. So, the impermeability condition is satisfied within the model.) The normal force, axial force and side force are then found from involved integrals by using Maple software, and the results are discussed.

2. Statement of problem

The steady and incompressible Navier–Stokes equations are given by (p. 577 of [17])

$$\rho u_j^\dagger \frac{\partial u_i^\dagger}{\partial x_j} = \frac{\partial p^\dagger}{\partial x_i} + \mu \frac{\partial^2 u_i^\dagger}{\partial x_j \partial x_j}, \quad \frac{\partial u_j^\dagger}{\partial x_j} = 0 \tag{1}$$

in the Cartesian coordinate system (x_1, x_2, x_3), with i and j integers such that $1 \leq i, j \leq 3$; a repeated suffix within a particular term implies a summation over the suffix values, for example $a_i b_i = a_1 b_1 + a_2 b_2 + a_3 b_3$. The Navier–Stokes velocity and pressure are $u_j^\dagger$ and $p^\dagger$ respectively. The fluid density and the dynamical coefficient of viscosity are ρ and μ respectively and are both assumed to be constant. The gradient operator is denoted by $\frac{\partial}{\partial x_j}$, and the Laplacian operator by $\frac{\partial^2}{\partial x_j \partial x_j}$. The Euler equations are then obtained by setting the viscosity μ to zero. This gives

$$\rho u_j \frac{\partial u_i}{\partial x_j} = \frac{\partial p}{\partial x_i}, \quad \frac{\partial u_j}{\partial x_j} = 0 \tag{2}$$

for the Euler velocity and pressure u_i and p respectively.

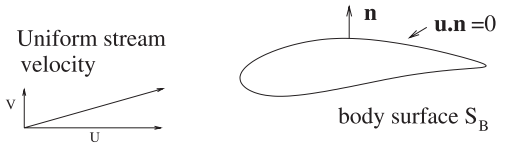

Figure 1. Body in a uniform flow field.

2.1 *Bernouilli and Laplace equations*

Assume that the flow is represented by a potential velocity φ such that $u_i = \frac{\partial \varphi}{\partial x_i}$. Then (2) reduces to

$$p + \frac{1}{2}\rho \frac{\partial \varphi}{\partial x_i}\frac{\partial \varphi}{\partial x_i} = p_0, \quad \frac{\partial^2 \varphi}{\partial x_j \partial x_j} = 0, \tag{3}$$

where p_0 is a constant. These equations are the Bernoulli equation for pressure p and Laplace equation for potential velocity φ respectively.

2.2 *Boundary conditions*

Consider uniform flow $(U, V, 0)$ past a fixed closed body of surface S_B such that the slip boundary condition

$$\vec{\mathbf{u}} \cdot \vec{\mathbf{n}} = \nabla \varphi \cdot \vec{\mathbf{n}} = \frac{\partial \varphi}{\partial \vec{\mathbf{n}}} = u_j n_j = 0 \tag{4}$$

holds on the body surface S_B, where $\vec{\mathbf{n}} = (n_1, n_2, n_3)$ is the outward pointing normal to the body surface S_B and $\vec{\mathbf{u}} = \nabla \varphi$ is the fluid velocity (figure 1).

Let the velocity $\vec{\mathbf{u}}^*$ be the perturbation velocity to the uniform stream $(U, V, 0)$. Then $\vec{\mathbf{u}} = \nabla \varphi = U\hat{\mathbf{x}}_\mathbf{1} + V\hat{\mathbf{x}}_\mathbf{2} + \vec{\mathbf{u}}^*$, where $\hat{\mathbf{x}}_\mathbf{1}$ and $\hat{\mathbf{x}}_\mathbf{2}$ are the unit vectors in the 1 and 2 directions respectively. The potential φ is then given by

$$\varphi = Ux_1 + Vx_2 + \varphi^* \tag{5}$$

where $\vec{\mathbf{u}}^* = \nabla \varphi^*$. The velocity is $u_i = \left(\delta_{i1}U + \delta_{i2}V + \frac{\partial \varphi^*}{\partial x_i}\right)$, and $\vec{\mathbf{u}}^* \to 0$ as $R \to \infty$, where the radius $R = \sqrt{x_1^2 + x_2^2 + x_3^2}$.

2.3 *Force integral*

The force on the body due to the fluid is represented by a surface integral of the normal pressure over the body surface [17] such that

$$\vec{\mathbf{F}} = -\int_{S_\mathrm{B}} p\vec{\mathbf{n}}\mathrm{d}s. \tag{6}$$

Let the force $\vec{\mathbf{F}} = (F_1, F_2, F_3)$, and replace p by the Bernoulli equation (3). Applying the divergence theorem then gives

$$F_i = -\int_{S_\mathrm{B}} pn_i \mathrm{d}s = \frac{1}{2}\rho \int_{S_\mathrm{B}} (u_j u_j) n_i \mathrm{d}s. \tag{7}$$

Making use of the slip (impermeability) boundary condition, (7) can be rewritten as

$$F_i = \frac{1}{2}\rho \int_{S_B} \{(u_j u_j)n_i - 2(u_i u_j n_j)\} \mathrm{d}s. \tag{8}$$

3. Body force induced by an infinitesimal horseshoe vortex

In this section, we describe an infinitesimal horseshoe vortex, and the force contribution it induces on the wing.

3.1 *Infinitesimal horseshoe vortex*

Model the flow by the standard textbook approach given in Lighthill (§11 of [18]) by a distribution of horseshoe vortices. This is represented pictorially by figure 2, where t denotes time. As the steady state $t \to \infty$ is approached, the closed circulation loops become horseshoe vortices. These vortices are aligned such that their span is in the x_3 direction and their trailing arms are in the x_1 direction.

Consider the horseshoe vortex consisting of the three vortex lines from $(\infty, 0, s)$ to $(0, 0, s)$, from $(0, 0, s)$ to $(0, 0, 0)$ and from $(0, 0, 0)$ to $(\infty, 0, 0)$ as shown in figure 3.

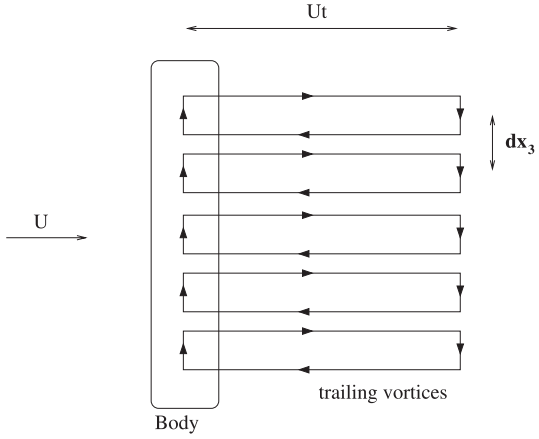

Figure 2. Pictorial representation of a wing by a finite distribution of horseshoe vortices.

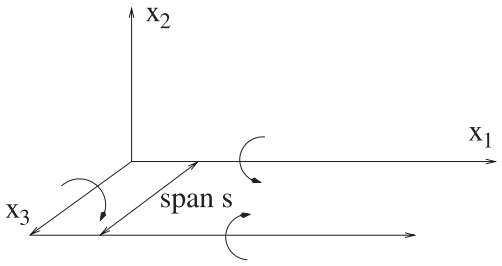

Figure 3. Horseshoe vortex.

The velocity of the horseshoe vortex [9] is given by

$$u_i = \frac{-\Gamma}{4\pi}\int_s^\infty \delta_{k1}\epsilon_{ijk}\frac{\partial}{\partial x_j}\left(\frac{1}{\{(x_1-\xi)^2+x_2^2+(x_3-s)^2\}^{\frac{1}{2}}}\right)\mathrm{d}\,\xi$$
$$+\frac{\Gamma}{4\pi}\int_0^\infty \delta_{k1}\epsilon_{ijk}\frac{\partial}{\partial x_j}\left(\frac{1}{\{(x_1-\xi)^2+x_2^2+x_3^2\}^{\frac{1}{2}}}\right)\mathrm{d}\,\xi$$
$$-\frac{\Gamma}{4\pi}\int_0^s \delta_{k3}\epsilon_{ijk}\frac{\partial}{\partial x_j}\left(\frac{1}{\{x_1^2+x_2^2+(x_3-\xi)^2\}^{\frac{1}{2}}}\right)\mathrm{d}\,\xi, \tag{9}$$

where s is the span and Γ is the circulation around the line vortex; $\delta_{ij} = 1$ for $i = j$ and zero otherwise; $\epsilon_{ijk} = 1$ for $(i, j, k) = (1, 2, 3)$, $(2, 3, 1)$ or $(3, 1, 2)$, $\epsilon_{ijk} = -1$ for $(i, j, k) = (1, 3, 2)$, $(2, 1, 3)$ or $(3, 2, 1)$, and $\epsilon_{ijk} = 0$ otherwise. In the limit as the span s tends to zero, the infinitesimal horseshoe vortex is obtained. This is given by Thwaites (p. 391, eq. (76) of [23]) as

$$\varphi* = \frac{Q}{2\pi}\frac{x_2}{r^2}\left(1+\frac{x_1}{\sqrt{x_1^2+r^2}}\right), \tag{10}$$

where the two-dimensional radius is given by $r = \sqrt{x_2^2+x_3^2}$ and $Q = \Gamma s/2$ is the strength (see [9]). Rearranging terms by noting that $R = \sqrt{x_1^2+r^2}$ and $(R+x_1)(R-x_1) = R^2 - x_1^2 = r^2$ gives

$$\varphi* = \frac{Q}{2\pi}\frac{x_2}{R(R-x_1)} = \frac{Q}{2\pi}\frac{\partial}{\partial x_2}\ln(R-x_1), \tag{11}$$

and so $\varphi*$ is the potential part of the lift oseenlet [16, 19] with lift $L = \rho U\Gamma s$; the lift oseenlet is normalized by taking $L = 1$. We note that the lift oseenlet is a fundamental solution providing a unit force at its origin. A span-wise distribution of these produces a potential equivalent to that for a flat vortex sheet, and consequently the force impulse acts on the bound vortex line, and not along the vortex sheet itself (in which case there would be no steady solution as the vortex sheet would move).

3.2 *Integral representation for the force induced by an infinitesimal horseshoe vortex*

Consider the force contribution from a single infinitesimal horseshoe vortex. The wing is constructed from an integral distribution of these, and the lift is given by the summation of all the contributions. The force integral over the body surface S_B can be replaced by an integral over the circular cylindrical surface S_C and a spherical surface S_R defined next.

The circular cylindrical surface S_C begins at the trailing edge, encompasses the singular lifting element line and ends at a large spherical radius distance R in the far downstream wake. Let the radius of the circular cylinder $\epsilon > 0$ be small, and so the surface S_C is defined along $x_2^2 + x_3^2 = \epsilon^2$, where $a \le x_1 \le \sqrt{R^2-\epsilon^2}$ and the trailing edge is positioned at $x_1 = a$.

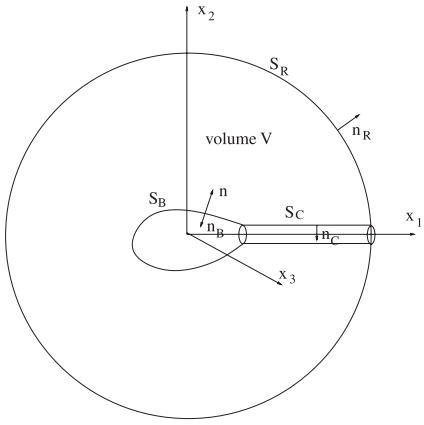

Figure 4. Singularity about x_1-axis.

The spherical surface S_{R} is centred on the body and is such that the radius $R \to \infty$ and on this surface $x_1^2 + x_2^2 + x_3^2 = R^2$ and $-R \le x_1 \le \sqrt{R^2 - \epsilon^2}$.

The body surface S_{B} can be replaced by the two surfaces S_{C} and S_{R} in the integral representation for the force because the resulting volume integral V which is contained within the surfaces S_{B}, S_{C} and S_{R} gives no contribution (see figure 4).

This is shown next by applying the divergence theorem such that (8) becomes

$$
\begin{aligned}
F_i &= \frac{1}{2}\rho \int_{S_{\mathrm{B}}} \{u_j u_j n_i - 2u_i u_j n_j\}\mathrm{d}s \\
&= -\frac{1}{2}\rho \int_{S_{\mathrm{B}}} \{u_j u_j (n_i)_{\mathrm{B}} - 2u_i u_j (n_j)_{\mathrm{B}}\}\mathrm{d}s \\
&= -\frac{1}{2}\rho \left\{ \int_V \left\{ \frac{\partial}{\partial x_i}\left(\frac{\partial \varphi}{\partial x_j}\frac{\partial \varphi}{\partial x_j}\right) - 2\frac{\partial}{\partial x_j}\left(\frac{\partial \varphi}{\partial x_i}\frac{\partial \varphi}{\partial x_j}\right)\right\} \mathrm{d}v \right. \\
&\quad + \int_{S_{\mathrm{R}}} \{u_j u_j (n_i)_{S_{\mathrm{R}}} - 2u_i u_j (n_j)_{\mathrm{R}}\}\mathrm{d}s \\
&\quad \left. + \int_{S_{\mathrm{C}}} \{u_j u_j (n_i)_{S_{\mathrm{C}}} - 2u_i u_j (n_j)_{\mathrm{C}}\}\mathrm{d}s \right\}, \qquad (12)
\end{aligned}
$$

where $\vec{\mathbf{n}}$ is the outward pointing normal to the body surface, $\vec{\mathbf{n_B}}$ is the inward pointing normal to the body surface and so $\vec{\mathbf{n}} = -\vec{\mathbf{n_B}}$. The normal $\vec{\mathbf{n_C}}$ points into the body surface S_{C} and the normal $\vec{\mathbf{n_R}}$ points outwards to the body surface S_{R}. However, from the Laplace equation we have $\frac{\partial}{\partial x_i}\left(\frac{\partial \varphi}{\partial x_j}\frac{\partial \varphi}{\partial x_j}\right) - 2\frac{\partial}{\partial x_j}\left(\frac{\partial \varphi}{\partial x_i}\frac{\partial \varphi}{\partial x_j}\right) = 0$. Therefore,

$$
\begin{aligned}
F_i = \frac{1}{2}\rho \left(\int_{S_{\mathrm{R}}} \{u_j u_j (n_i)_{S_{\mathrm{R}}} - 2u_i u_j (n_j)_{S_{\mathrm{R}}}\}\mathrm{d}s \right. \\
\left. + \int_{S_{\mathrm{C}}} \{u_j u_j (n_i)_{S_{\mathrm{C}}} - 2u_i u_j (n_j)_{S_{\mathrm{C}}}\}\mathrm{d}s \right). \qquad (13)
\end{aligned}
$$

Table 1. Symmetry properties of partial differentials of φ^*.

Symmetry	$\frac{\partial\varphi^*}{\partial x_1}$	$\frac{\partial\varphi^*}{\partial x_2}$	$\frac{\partial\varphi^*}{\partial x_3}$
In terms of x_1	even	none	none
In terms of x_2	odd	even	odd
In terms of x_3	even	even	odd

For the sake of simplicity, we denote the common integrand by

$$\textbf{Integrand}(F_i) = \{u_j u_j n_i - 2u_i u_j n_j\}.$$

This integrand is non-linear, and is expanded such that each term is evaluated individually using Maple. The results of these are given in Appendix B.

3.3 *Useful properties simplifying analysis*

We employ two useful properties, symmetry of the integrand and some harmonic properties of functions, to simplify the analysis. These properties are then used to evaluate the forces on the body.

3.3.1 *Symmetry.* Since the surface S_{R} is symmetric with respect to the x_1x_3 or x_1x_2 planes, $\int_{S_{\mathrm{R}}} g\mathrm{d}s = 0$ if g is an antisymmetric function in terms of x_2 or x_3. Also, if g is a symmetric (even) function in terms of x_2, then its derivative with respect to x_2 will be an antisymmetric (odd) function in terms of x_2 (and vice versa). For example, $\frac{\partial}{\partial x_2}\log\left(\sqrt{x_1^2+x_2^2+x_3^2}-x_1\right)$ is an antisymmetric function in terms of x_2 because $\log\left(\sqrt{x_1^2+x_2^2+x_3^2}-x_1\right)$ is a symmetric function in terms of x_2. We summarize these results for φ^* given by (11) in table 1.

3.3.2 *Harmonics.* Simple computations show that $\frac{\partial^2}{\partial x_1^2}\log(R-x_1) = -\frac{x_1}{R^3}$, $\frac{\partial^2}{\partial x_2^2}\log(R-x_1) = \frac{R^3-R^2x_1-x_2(2x_2R-x_1x_2)}{R^3(R-x_1)^2}$ and $\frac{\partial^2}{\partial x_3^2}\log(R-x_1) = \frac{R^3-R^2x_1-x_3(2x_3R-x_1x_3)}{R^3(R-x_1)^2}$. So,

$$\left(\frac{\partial^2}{\partial x_1^2}+\frac{\partial^2}{\partial x_2^2}+\frac{\partial^2}{\partial x_3^2}\right)\log(R-x_1) = \nabla^2\log(R-x_1) = 0. \tag{14}$$

Since $\log(R-x_1)$ is harmonic, so are $\frac{\partial}{\partial x_1}\log(R-x_1)$ and $\frac{\partial}{\partial x_2}\log(R-x_1)$ in the same region. So,

$$\nabla^2\frac{\partial}{\partial x_1}\log(R-x_1) = 0\ ,\ \text{and}\ \nabla^2\frac{\partial}{\partial x_2}\log(R-x_1) = 0. \tag{15}$$

4. Axial force

We calculate the contribution to the axial force from the lifting element. First consider the contribution over the spherical surface S_{R}. The integrand is given by (B2) in Appendix B, and each term is calculated in turn using Maple software [2], the results

given in Appendix C. Next we calculate the contribution to the axial force from the lifting element over the cylindrical surface S_C. The integrand is given by (B5) in Appendix B, and each term is calculated in turn using Maple software [2], the results given in Appendix D. Combining all the results together from Appendices B, C and D we get

$$\begin{aligned}\mathbf{F}_1 &= \lim_{\epsilon\to 0}\left\{\frac{1}{2}\rho\left(\int_{S_R}\mathbf{Integrand}(F_1)_{S_R}+\int_{S_C}\mathbf{Integrand}(F_1)_{S_C}\mathrm{d}s\right)\right\}\\ &= -\frac{1}{2}\frac{V}{U}+\frac{1}{32\rho\pi U^2R^2}-\frac{1}{16a^2\rho\pi U^2}\\ &\quad+\lim_{\epsilon\to 0}\left\{\frac{1}{32R(a^2+\epsilon^2)^{\frac{5}{2}}\rho\epsilon^2\pi U^2}\right.\\ &\quad\times\{2\sqrt{a^2+\epsilon^2}R\epsilon^4+2\sqrt{R^2-\epsilon^2}\sqrt{a^2+\epsilon^2}\epsilon^4+3\epsilon^2a^3R\\ &\quad+\sqrt{R^2-\epsilon^2}\sqrt{a^2+\epsilon^2}a^2\epsilon^2+4\sqrt{a^2+\epsilon^2}Ra^2\epsilon^2+4a^5R\\ &\quad\left.-2\sqrt{R^2-\epsilon^2}a^4\sqrt{a^2+\epsilon^2}+2\sqrt{a^2+\epsilon^2}Ra^4\}\right\}.\end{aligned}$$

However, since $-2\sqrt{R^2-\epsilon^2}a^4\sqrt{a^2+\epsilon^2}+2\sqrt{a^2+\epsilon^2}Ra^4 = 2a^4\sqrt{a^2+\epsilon^2}(R-\sqrt{R^2-\epsilon^2})>0$, then $\mathbf{F}_1$ is of order $O(\frac{1}{\epsilon^2})$ and tends to infinity as $\epsilon\to 0$. So $\mathbf{F}_1\to+\infty$.

5. Normal force

Similarly, we calculate the contribution to the normal force from the infinitesimal horseshoe vortex. First consider the contribution over the spherical surface S_R. The integrand is given by (B3) in Appendix B, and each term is calculated in turn. These evaluations are determined using Maple software [2], and given in Appendix E. Second, we calculate the contribution to the normal force from the lifting element over the cylindrical surface S_C. The integrand is given by (B6), and the calculation of each term in turn is given in Appendix E. Combining all the results together gives

$$\begin{aligned}\mathbf{F}_2 &= \lim_{\epsilon\to 0}\left\{\frac{1}{2}\rho\left(\int_{S_R}\mathbf{Integrand}(F_2)_{S_R}+\int_{S_C}\mathbf{Integrand}(F_2)_{S_C}\mathrm{d}s\right)\right\}\\ &= \lim_{\epsilon\to 0}\left\{\frac{1}{2}\rho\left(2\epsilon^2UV\pi+\frac{2}{3\rho}+\frac{1}{3\rho}-\frac{1}{2\rho}\frac{(\sqrt{R^2-\epsilon^2}\sqrt{a^2+\epsilon^2}-aR)}{R\sqrt{a^2+\epsilon^2}}\right)\right\}=\frac{1}{2}.\end{aligned}$$

Hence, the normal force is a half, which is the same as and confirms the result given in [9].

6. Side force

In this case the whole integrand given in (B4) over S_R, and the integrand given in (B7) over S_C are antisymmetric in terms of x_3. Although there is an additional contribution over the surface generated by the intersection of the surfaces S_R and S_C which breaks the

symmetry, we show in Appendix F that this contribution is zero and so can be ignored. The remaining contribution is then

$$\mathbf{F}_3 = \left\{ \frac{1}{2}\rho \left(\int_{S_\mathrm{R}} \mathbf{Integrand}(F_2)_{S_\mathrm{R}} + \int_{S_\mathrm{C}} \mathbf{Integrand}(F_2)_{S_\mathrm{C}} \mathrm{d}s \right) \right\} = 0.$$

7. Discussion

Workers in the field recognize that the traditional inviscid flow representation, which includes the impermeability boundary condition and the application of the Kutta condition at the trailing edge, is an approximation aimed at incorporating viscous effects or other subliminal effects. However, the inviscid representation assumes that any viscous terms are bounded such that for large Reynolds number they are small and can be ignored, leading to an inviscid Euler flow representation. This holds for two-dimensional flows which includes thin aerofoil theory and triple-deck theories which are presented in two-dimensions. However, in three-dimensional flow Goldstein (pp. 131–134 of [13]) challenges the view that viscosity is bounded, and suggests that instead the appropriate model incorporates viscous diffusion even for vanishing boundary layer thickness. This is supported by the far-field Oseen flow description, for which the general Oseen flow representation contains singular and coupled inviscid-viscous terms. Even for large Reynolds number, the viscous terms cannot be assumed to be bounded and small [7, 24]. This view is supported in this paper, where we find that these viscous terms are necessary not only for the correct evaluation of the normal force as was shown in the author's previous papers [9, 6], but also for the correct evaluation of the axial force. Omitting them in an Euler model leads to unphysical evaluations for the forces on the body. In particular, it is shown that the normal force contribution from inviscid terms is half the total, and the axial force is infinite which are both unphysical results. This is in contrast to the generally accepted result for Euler flow, that the normal force contribution from inviscid terms is not reduced by half and the axial force is not infinite. However, this generally accepted result relies upon fortuitously omitting the force contribution at the trailing edge due to the singular pressure field. This oversight is incorrect [9] but fortuitous, because there is no additional force contribution at the trailing edge if the viscous forces are included in the model because they remove the artificial singularities and so regularize the flow field. However, only by including viscosity into the model can it be argued that there is no additional force across the trailing edge. This provides further evidence that the ideal Navier–Stokes limit for this problem is a modified Euler flow which includes singular viscous terms residing in the vortex wake that do not tend to zero for large Reynolds number.

The inclusion of the viscous term has important implications in the calculation of the lift force for slender bodies. Presently, the viscous cross-flow contribution is calculated experimentally from a semi-empirical method devised by Allen and Perkins [1]. However, it is shown that this additional viscous contribution can be calculated within a theoretical model by means of a slender body Oseen flow theory [8, 5].

Recognizing the limitations of the Euler model presented here enable the development of new models for the future, and demonstrates the practical as well as theoretical importance of not neglecting the viscous terms. For example, consider triple-deck theory [21, 22] in a two-dimensional flow. An outer inviscid flow is assumed which is then matched through subsequent asymptotic viscous layers to the boundary. One can then move back up through the layers to get a bounded correction to the outer inviscid flow field. However, extending

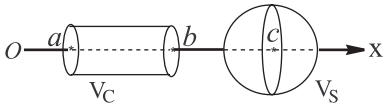

Figure 5. Cylinder V_C and sphere V_S.

this to the three-dimensional lifting wing problem, the work in this paper demonstrates that the outer layer is not purely inviscid, but also incorporates a coupled counter-balancing viscous term to the singular inviscid term that is also singular (unbounded) such that the resulting combined flow field is bounded. The coupled unbounded viscous term is intrinsic to the initial outer flow representation and so extending triple-deck theory for three-dimensional flow problems requires this term to be included. It is noted that this viscous term is different from the bounded correction obtained by moving up the triple-deck layers. This point has already been made in [6] and work is on-going to develop an extension of triple deck theory for three-dimensional flow problems which includes this outer viscous term.

Appendix

Appendix A: *Kinetic energy calculation*

We present the computation of the kinetic energy

$$KE = \frac{1}{2}\rho \int_V \nabla\varphi \cdot \nabla\varphi \mathrm{d}v \tag{A1}$$

for the potential $\varphi^*(x_1, x_2, x_3) = \frac{1}{4\pi\rho U}\frac{\partial}{\partial x_2}\log\left(\sqrt{x_1^2 + x_2^2 + x_3^2} - x_1\right)$ where V is:

(1) a cylinder of volume V_C with radius ϵ along the x_1-axis where, $0 < a \le x_1 \le b$;
(2) a sphere of volume V_S and radius R, with centre lying on the x_1-axis at point $(c, 0, 0)$ where $c > 2R$ (figure 5).

Let $M > 1$ be any real number. We show that $KE > M$, and since M is arbitrary then $KE \to +\infty$. We note that $\nabla\varphi \cdot \nabla\varphi \ge \left(\frac{\partial\varphi^*}{\partial x_1}\right)^2 = \left(\frac{1}{4\pi\rho U}\frac{x_2}{R^3}\right)^2$, which shall be used in the following evaluation.

(1) *Computing the kinetic energy within the volume* V_C. The volume V_C is defined such that $x_2^2 + x_3^2 \le \epsilon^2$, $0 < a \le x_1 \le b$. Let $x_2 = r\cos\phi$, $x_3 = r\sin\phi$ and $0 \le \phi \le 2\pi$, $0 \le r \le \epsilon$. Consider $0 < \delta < \sqrt{\frac{A\epsilon^2}{A + M\epsilon^2}}$, where $A = \frac{(b-a)}{64\pi\rho U^2}$. Then $\frac{(b-a)}{32\pi\rho^2U^2}\frac{-\delta^2+\epsilon^2}{\epsilon^2\delta^2} > \frac{2M}{\rho}$. This implies

$$\begin{aligned} KE|_{V_C} &= \frac{\rho}{2}\int_{V_C} \nabla\varphi \cdot \nabla\varphi \mathrm{d}v \ge \frac{\rho}{2}\int_{V_C}\left(\frac{\partial\varphi^*}{\partial x_1}\right)^2 \mathrm{d}v \\ &= \frac{\rho}{2}\int_0^{\epsilon}\int_a^b\int_0^{2\pi}\left(\frac{\partial\varphi^*}{\partial x_1}\right)^2 r\,\mathrm{d}\phi\,\mathrm{d}x_1\,\mathrm{d}r \\ &\ge \frac{\rho}{2}\int_{\delta}^{\epsilon}\int_a^b\int_0^{2\pi}\left(\frac{\partial\varphi^*}{\partial x_1}\right)^2 r\,\mathrm{d}\phi\,\mathrm{d}x_1\,\mathrm{d}r \end{aligned}$$

$$= \frac{\rho}{2}\int_{\delta}^{\epsilon}\left(\int_{a}^{b}\left(\int_{0}^{2\pi}\left(\frac{\cos^2\phi}{16\pi^2\rho^2U^2r^4}\right)\mathrm{d}\,\phi\right)\mathrm{d}x_1\right)r\,\mathrm{d}\,r$$

$$= \frac{\rho}{2}\left(\frac{(b-a)}{32\pi\rho^2U^2}\frac{-\delta^2+\epsilon^2}{\epsilon^2\delta^2}\right) > M,$$

and so $KE|_{V_C} \to +\infty$.

(2) *Computing the kinetic energy within the volume* V_S. The volume V_S is defined by $(x_1-c)^2+x_2^2+x_3^2 \le R^2$, where $x_1 = c + h\cos\theta$, $x_2 = h\sin\theta\cos\phi$, and $x_3 = h\sin\theta\sin\phi$, $0 \le \theta \le \pi$, $0 \le \phi \le 2\pi$, $0 \le h \le R$. Consider $0 < \delta < \frac{AR}{A+RM}$, where $A = \frac{1}{24\pi\rho U^2}$, then $\frac{1}{12\pi\rho^2U^2}\frac{R-\delta}{R\delta} > \frac{2M}{\rho}$. This implies

$$KE|_{V_S} = \frac{\rho}{2}\int_{V_S}\nabla\varphi\cdot\nabla\varphi\mathrm{d}v \ge \frac{\rho}{2}\int_{V_S}\left(\frac{\partial\varphi^*}{\partial x_1}\right)^2\mathrm{d}v$$

$$= \frac{\rho}{2}\int_0^R\int_0^\pi\int_0^{2\pi}\left(\frac{\partial\varphi^*}{\partial x_1}\right)^2 h^2\sin\theta\mathrm{d}\,\phi\mathrm{d}\theta\mathrm{d}h$$

$$\ge \frac{\rho}{2}\int_\delta^R\int_0^\pi\int_0^{2\pi}\left(\frac{\partial\varphi^*}{\partial x_1}\right)^2 h^2\sin\theta\mathrm{d}\,\phi\mathrm{d}\theta\mathrm{d}h$$

$$= \frac{\rho}{2}\int_\delta^R\left(\int_0^\pi\left(\int_0^{2\pi}\left(\frac{\sin^2\theta\cos^2\phi}{16\pi^2\rho^2U^2h^4}\right)\mathrm{d}\,\phi\right)\sin\theta d\theta\right)h^2\mathrm{d}h$$

$$= \frac{\rho}{2}\left(\frac{1}{12\pi\rho^2U^2}\frac{R-\delta}{R\delta}\right) > M,$$

and so $KE|_{V_S} \to +\infty$.

We now compute the kinetic energy of the fluid exterior to the body surface S_B due to the presence of a single infinitesimal horseshoe vortex. The potential is ϕ^*, and the total fluid volume V is considered (see figure 4). The kinetic energy within this volume is larger than the kinetic energy within the volume V_{R-r}, as shown in figure 6; the volume V_{R-r} is the volume inside the sphere S_R and outside the sphere S_r of radius r. This volume excludes

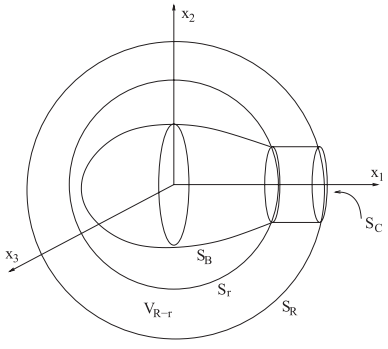

Figure 6. Volume V_{R-r}.

the cylinder S_C, and so $S_B \subset V_{R-r} \subset V$. The volume V_{R-r} is included in the domain $\alpha \leq \theta \leq 2\pi$ where $\alpha = \arccos\left(\frac{\sqrt{R^2-\epsilon^2}}{R}\right)$ is the angle subtended by the intersection of the surfaces S_R and S_C.

The kinetic energy is then

$$
\begin{aligned}
KE|_V &\geq KE|_{V_{R-r}} \\
&= \frac{\rho}{2}\int_{V_{R-r}} \nabla\varphi \cdot \nabla\varphi \mathrm{d}v \\
&\geq \frac{\rho}{2}\int_{V_{R-r}} \left(\frac{\partial\varphi^*}{\partial x_2}\right)^2 \mathrm{d}v = \frac{\rho}{2}\int_r^R \int_\alpha^\pi \int_0^{2\pi} \left(\frac{\partial\varphi^*}{\partial x_2}\right)^2 h^2 \sin\theta \mathrm{d}\phi \mathrm{d}\theta \mathrm{d}h \\
&= \frac{\rho}{2}\int_r^R \left(\int_\alpha^\pi \left(\int_0^{2\pi} \left(-\frac{1}{4}\frac{\cos^2\phi\cos^2\theta - \cos^2\phi\cos\theta + 1 - 2\cos^2\phi}{(-1+\cos\theta)\pi\rho U h^2}\right)^2 \mathrm{d}\phi\right)\right. \\
&\quad \left. \times \sin^3\theta \mathrm{d}\theta\right) h^2 \mathrm{d}h \\
&= \frac{1}{240}\frac{R-r}{\pi\rho^2 U^2 R r}\cos^{10}\frac{1}{2}\alpha \left\{30\ln\left(1+\tan^2\frac{1}{2}\alpha\right) - 60\ln\left(\tan\frac{1}{2}\alpha\right)\right. \\
&\quad - 115\tan^2\frac{1}{2}\alpha - 17 - 245\tan^4\frac{1}{2}\alpha - 105\tan^6\frac{1}{2}\alpha - 30\tan^8\frac{1}{2}\alpha \\
&\quad - 300\ln\left(\tan\frac{1}{2}\alpha\right)\tan^2\frac{1}{2}\alpha - 600\ln\left(\tan\frac{1}{2}\alpha\right)\tan^4\frac{1}{2}\alpha \\
&\quad - 600\ln\left(\tan\frac{1}{2}\alpha\right)\tan^6\frac{1}{2}\alpha - 300\ln\left(\tan\frac{1}{2}\alpha\right)\tan^8\frac{1}{2}\alpha \\
&\quad - 60\ln\left(\tan\frac{1}{2}\alpha\right)\tan^{10}\frac{1}{2}\alpha + 150\ln\left(1+\tan^2\frac{1}{2}\alpha\right)\tan^2\frac{1}{2}\alpha \\
&\quad + 300\ln\left(1+\tan^2\frac{1}{2}\alpha\right)\tan^4\frac{1}{2}\alpha + 300\ln\left(1+\tan^2\frac{1}{2}\alpha\right)\tan^6\frac{1}{2}\alpha \\
&\quad \left. + 150\ln\left(1+\tan^2\frac{1}{2}\alpha\right)\tan^8\frac{1}{2}\alpha + 30\ln\left(1+\tan^2\frac{1}{2}\alpha\right)\tan^{10}\frac{1}{2}\alpha\right\} = I(\alpha). \qquad \text{(A2)}
\end{aligned}
$$

We have used the result that $\ln\left(\tan\frac{1}{2}\alpha\right)\tan^m\frac{1}{2}\alpha \approx \left(\frac{\alpha}{2}\right)^m \ln\left(\frac{1}{2}\alpha\right)$ as $\alpha \to 0^+$, and $\lim_{\alpha\to 0}\left(\frac{\alpha}{2}\right)^m \ln\left(\frac{1}{2}\alpha\right) = \lim_{\alpha\to 0}\left(-\frac{\alpha^m}{m2^m}\right) = 0$ for all positive values of m. This means that the dominant term in the solution of $I(\alpha)$) is $-60\ln\left(\tan\frac{1}{2}\alpha\right)$. So

$$\lim_{\alpha\to 0} I(\alpha) = \lim_{\alpha\to 0}\frac{1}{240}\frac{R-r}{\pi\rho^2 U^2 R r}\cos^{10}\left(\frac{1}{2}\alpha\right)\left(-60\ln\left(\tan\frac{1}{2}\alpha\right)\right) = +\infty.$$

This is sufficient to show that the kinetic energy of the system is unbounded, since

$$KE|_V \geq \lim_{\alpha\to 0} KE|_{V_{R-r}} = +\infty.$$

Appendix B: *The expansion of the force integrand*

This integrand is non-linear, and is expanded such that each term is evaluated individually using Maple. The force is given in §3.2 as

$$F_i = \frac{1}{2}\rho\left(\int_{S_R} \textbf{Integrand}(F_i)_{S_R}\,\mathrm{d}s + \int_{S_C} \textbf{Integrand}(F_i)_{S_C}\,\mathrm{d}s\right). \tag{B1}$$

We have

$$\begin{aligned}
&\{u_j u_j n_i - 2u_i u_j n_j\}\\
&= \left\{\left(U^2+V^2+2U\frac{\partial\varphi^*}{\partial x_1}+2V\frac{\partial\varphi^*}{\partial x_2}+\nabla\varphi^*\cdot\nabla\varphi^*\right)n_i\right.\\
&\quad \left.-2\left(\delta_{i1}U+\delta_{i2}V+\frac{\partial\varphi^*}{\partial x_i}\right)\left(\delta_{j1}U+\delta_{j2}V+\frac{\partial\varphi^*}{\partial x_j}\right)n_j\right\}\\
&= \left\{\left(U^2+V^2+2U\frac{\partial\varphi^*}{\partial x_1}+2V\frac{\partial\varphi^*}{\partial x_2}+\nabla\varphi^*\cdot\nabla\varphi^*\right)n_i\right.\\
&\quad -2\left[\left(\delta_{i1}U^2+\delta_{i2}UV+U\frac{\partial\varphi^*}{\partial x_i}\right)n_1+\left(\delta_{i2}V^2+\delta_{i1}UV+V\frac{\partial\varphi^*}{\partial x_i}\right)n_2\right.\\
&\quad \left.\left.+\left(\delta_{i1}U\frac{\partial\varphi^*}{\partial x_j}+\delta_{i2}V\frac{\partial\varphi^*}{\partial x_j}+\frac{\partial\varphi^*}{\partial x_i}\frac{\partial\varphi^*}{\partial x_j}\right)n_j\right]\right\}.
\end{aligned}$$

So,

$$\begin{aligned}
&\textbf{Integrand}(\mathbf{F}_1)\\
&=\left(-U^2+V^2-2U\frac{\partial\varphi^*}{\partial x_1}+2V\frac{\partial\varphi^*}{\partial x_2}-\left(\frac{\partial\varphi^*}{\partial x_1}\right)^2+\left(\frac{\partial\varphi^*}{\partial x_2}\right)^2+\left(\frac{\partial\varphi^*}{\partial x_3}\right)^2\right)n_1\\
&\quad -2\left(UV+U\frac{\partial\varphi^*}{\partial x_2}+V\frac{\partial\varphi^*}{\partial x_1}+\frac{\partial\varphi^*}{\partial x_1}\frac{\partial\varphi^*}{\partial x_2}\right)n_2-2\left(U\frac{\partial\varphi^*}{\partial x_3}+\frac{\partial\varphi^*}{\partial x_1}\frac{\partial\varphi^*}{\partial x_3}\right)n_3,
\end{aligned}$$

$$\begin{aligned}
&\textbf{Integrand}(\mathbf{F}_2)\\
&= -2\left(UV+V\frac{\partial\varphi^*}{\partial x_1}+U\frac{\partial\varphi^*}{\partial x_2}+\frac{\partial\varphi^*}{\partial x_1}\frac{\partial\varphi^*}{\partial x_2}\right)n_1\\
&\quad +\left(U^2-V^2+2U\frac{\partial\varphi^*}{\partial x_1}-2V\frac{\partial\varphi^*}{\partial x_2}+\left(\frac{\partial\varphi^*}{\partial x_1}\right)^2-\left(\frac{\partial\varphi^*}{\partial x_2}\right)^2+\left(\frac{\partial\varphi^*}{\partial x_3}\right)^2\right)n_2\\
&\quad -2\left(V\frac{\partial\varphi^*}{\partial x_3}+\frac{\partial\varphi^*}{\partial x_2}\frac{\partial\varphi^*}{\partial x_3}\right)n_3, \quad \text{and}
\end{aligned}$$

Integrand$(\mathbf{F}_3)$

$$= -2\left(U\frac{\partial\varphi^*}{\partial x_3}+\frac{\partial\varphi^*}{\partial x_1}\frac{\partial\varphi^*}{\partial x_3}\right)n_1-2\left(V\frac{\partial\varphi^*}{\partial x_3}+\frac{\partial\varphi^*}{\partial x_2}\frac{\partial\varphi^*}{\partial x_3}\right)n_2$$

$$+\left(U^2+V^2+2U\frac{\partial\varphi^*}{\partial x_1}+2V\frac{\partial\varphi^*}{\partial x_2}+\left(\frac{\partial\varphi^*}{\partial x_1}\right)^2+\left(\frac{\partial\varphi^*}{\partial x_2}\right)^2-\left(\frac{\partial\varphi^*}{\partial x_3}\right)^2\right)n_3.$$

These integrals will be calculated in turn for each force component, using Maple. Over the surfaces S_{C} and S_{R}, the integrations then become:

*B*1 *Force components on* S_{R}

Integrand$(\mathbf{F}_1)_{S_{\mathrm{R}}}$

$$=\left(-U^2+V^2-2U\frac{\partial\varphi^*}{\partial x_1}+2V\frac{\partial\varphi^*}{\partial x_2}-\left(\frac{\partial\varphi^*}{\partial x_1}\right)^2+\left(\frac{\partial\varphi^*}{\partial x_2}\right)^2+\left(\frac{\partial\varphi^*}{\partial x_3}\right)^2\right)\left(\frac{x_1}{R}\right)$$

$$-2\left(UV+U\frac{\partial\varphi^*}{\partial x_2}+V\frac{\partial\varphi^*}{\partial x_1}+\frac{\partial\varphi^*}{\partial x_1}\frac{\partial\varphi^*}{\partial x_2}\right)\left(\frac{x_2}{R}\right)$$

$$-2\left(U\frac{\partial\varphi^*}{\partial x_3}+\frac{\partial\varphi^*}{\partial x_1}\frac{\partial\varphi^*}{\partial x_3}\right)\left(\frac{x_3}{R}\right), \tag{B2}$$

Integrand$(\mathbf{F}_2)_{S_{\mathrm{R}}}$

$$= -2\left(UV+V\frac{\partial\varphi^*}{\partial x_1}+U\frac{\partial\varphi^*}{\partial x_2}+\frac{\partial\varphi^*}{\partial x_1}\frac{\partial\varphi^*}{\partial x_2}\right)\left(\frac{x_1}{R}\right)$$

$$+\left(U^2-V^2+2U\frac{\partial\varphi^*}{\partial x_1}-2V\frac{\partial\varphi^*}{\partial x_2}+\left(\frac{\partial\varphi^*}{\partial x_1}\right)^2-\left(\frac{\partial\varphi^*}{\partial x_2}\right)^2+\left(\frac{\partial\varphi^*}{\partial x_3}\right)^2\right)\left(\frac{x_2}{R}\right)$$

$$-2\left(V\frac{\partial\varphi^*}{\partial x_3}+\frac{\partial\varphi^*}{\partial x_2}\frac{\partial\varphi^*}{\partial x_3}\right)\left(\frac{x_3}{R}\right), \tag{B3}$$

Integrand$(\mathbf{F}_3)_{S_{\mathrm{R}}}$

$$= -2\left(U\frac{\partial\varphi^*}{\partial x_3}+\frac{\partial\varphi^*}{\partial x_1}\frac{\partial\varphi^*}{\partial x_3}\right)\left(\frac{x_1}{R}\right)-2\left(V\frac{\partial\varphi^*}{\partial x_3}+\frac{\partial\varphi^*}{\partial x_2}\frac{\partial\varphi^*}{\partial x_3}\right)\left(\frac{x_2}{R}\right)$$

$$+\left(U^2+V^2+2U\frac{\partial\varphi^*}{\partial x_1}+2V\frac{\partial\varphi^*}{\partial x_2}+\left(\frac{\partial\varphi^*}{\partial x_1}\right)^2+\left(\frac{\partial\varphi^*}{\partial x_2}\right)^2-\left(\frac{\partial\varphi^*}{\partial x_3}\right)^2\right)\left(\frac{x_3}{R}\right). \tag{B4}$$

*B*2 *Force components on* S_{C}

$$\textbf{Integrand}(\mathbf{F}_1)_{S_{\mathrm{C}}}$$

$$= -2\left(UV + U\frac{\partial\varphi^*}{\partial x_2} + V\frac{\partial\varphi^*}{\partial x_1} + \frac{\partial\varphi^*}{\partial x_1}\frac{\partial\varphi^*}{\partial x_2}\right)\left(-\frac{x_2}{\epsilon}\right)$$

$$-2\left(U\frac{\partial\varphi^*}{\partial x_3} + \frac{\partial\varphi^*}{\partial x_1}\frac{\partial\varphi^*}{\partial x_3}\right)\left(-\frac{x_3}{\epsilon}\right), \tag{B5}$$

$$\textbf{Integrand}(\mathbf{F}_2)_{S_{\mathrm{C}}}$$

$$= \left(U^2 - V^2 + 2U\frac{\partial\varphi^*}{\partial x_1} - 2V\frac{\partial\varphi^*}{\partial x_2} + \left(\frac{\partial\varphi^*}{\partial x_1}\right)^2 - \left(\frac{\partial\varphi^*}{\partial x_2}\right)^2 + \left(\frac{\partial\varphi^*}{\partial x_3}\right)^2\right)\left(-\frac{x_2}{\epsilon}\right)$$

$$-2\left(V\frac{\partial\varphi^*}{\partial x_3} + \frac{\partial\varphi^*}{\partial x_2}\frac{\partial\varphi^*}{\partial x_3}\right)\left(-\frac{x_3}{\epsilon}\right), \tag{B6}$$

$$\textbf{Integrand}(\mathbf{F}_3)_{S_{\mathrm{C}}}$$

$$= -2\left(V\frac{\partial\varphi^*}{\partial x_3} + \frac{\partial\varphi^*}{\partial x_2}\frac{\partial\varphi^*}{\partial x_3}\right)\left(-\frac{x_2}{\epsilon}\right)$$

$$+\left(U^2 + V^2 + 2U\frac{\partial\varphi^*}{\partial x_1} + 2V\frac{\partial\varphi^*}{\partial x_2} + \left(\frac{\partial\varphi^*}{\partial x_1}\right)^2 + \left(\frac{\partial\varphi^*}{\partial x_2}\right)^2 - \left(\frac{\partial\varphi^*}{\partial x_3}\right)^2\right)\left(-\frac{x_3}{\epsilon}\right). \tag{B7}$$

Appendix C: *Evaluation of the axial force over the sphere* S_{R}

The following list of results have been obtained by Maple and used in the evaluation:

(1) $\int_{S_{\mathrm{R}}}\left\{\left(-2U\frac{\partial\varphi^*}{\partial x_1}\right)\frac{x_1}{R} + \left((-2UV) + \left(-2U\frac{\partial\varphi^*}{\partial x_2}\right)\right)\frac{x_2}{R} + \left(-2U\frac{\partial\varphi^*}{\partial x_3}\right)\frac{x_3}{R}\right\}\mathrm{d}s = 0$ because of antisymmetry of integrand in term of x_2.

(2) $\int_{S_{\mathrm{R}}}(-U^2 + V^2)\frac{x_1}{R}\mathrm{d}s = (U^2 - V^2)\pi\epsilon^2$.

(3) $\int_{S_{\mathrm{R}}}\left(-\left(\frac{\partial\varphi^*}{\partial x_1}\right)^2\right)\frac{x_1}{R}\mathrm{d}s = -\frac{1}{64R^6\pi\rho^2U^2}\epsilon^4$.

(4) $\int_{S_{\mathrm{R}}}\left(2V\frac{\partial\varphi^*}{\partial x_2}\right)\frac{x_1}{R}\mathrm{d}s = \frac{V}{2\pi\rho U}\int_{S_{\mathrm{R}}}\left(\frac{\partial^2}{\partial x_2^2}\left(\log(R - x_1)\right)\right)\frac{x_1}{R}\mathrm{d}s$

$$= \frac{V}{2\pi\rho U}\left(\frac{1}{2}\int_{S_{\mathrm{R}}}\left\{\left(\left(\frac{\partial^2}{\partial x_2^2} + \frac{\partial^2}{\partial x_3^2}\right)\log(R - x_1)\right)\frac{x_1}{R}\right\}\mathrm{d}s\right).$$

From (14) we have

$$\left(\frac{\partial^2}{\partial x_2^2} + \frac{\partial^2}{\partial x_3^2}\right)\log(R - x_1) = -\frac{\partial^2}{\partial x_1^2}\log(R - x_1) = \frac{x_1}{R^3},$$

so,

$$\int_{S_R}\left(2V\frac{\partial\varphi^*}{\partial x_2}\right)\frac{x_1}{R}\mathrm{d}s = -\frac{V}{4\pi\rho U}\int_{S_R}\frac{x_1^2}{R^4}\mathrm{d}s$$

$$= -\frac{V}{4\pi\rho U}\left(\frac{1}{3}\int_{S_R}\frac{x_1^2+x_2^2+x_3^2}{R^4}\mathrm{d}s\right) = -\frac{V}{3\rho U}.$$

Similarly,

(5) $\int_{S_R}\left(-2V\frac{\partial\varphi^*}{\partial x_1}\right)\frac{x_2}{R}\mathrm{d}s = -\frac{2V}{3\rho U}$.

(6) $\int_{S_R}\left(\left(\frac{\partial\varphi^*}{\partial x_2}\right)^2\right)n_1\mathrm{d}s = \frac{1}{16\epsilon^2\pi\rho^2U^2} + \frac{1}{16\epsilon^2R\pi\rho^2U^2}\sqrt{R^2-\epsilon^2} - \frac{3}{32R^2\pi\rho^2U^2}$
$-\frac{1}{16R^3\pi\rho^2U^2}\sqrt{R^2-\epsilon^2} + \frac{1}{128}\frac{\epsilon^2}{R^4\pi\rho^2U^2} + \frac{3}{256}\frac{\epsilon^4}{R^6\pi\rho^2U^2}$.

(7) $\int_{S_R}\left(\left(\frac{\partial\varphi^*}{\partial x_3}\right)^2\right)n_1\mathrm{d}s = \frac{1}{16\epsilon^2\pi\rho^2U^2} + \frac{1}{16R\epsilon^2\pi\rho^2U^2}\sqrt{R^2-\epsilon^2} - \frac{3}{32R^2\pi\rho^2U^2}$
$-\frac{1}{16R^3\pi\rho^2U^2}\sqrt{R^2-\epsilon^2} + \frac{3}{128R^4}\frac{\epsilon^2}{\pi\rho^2U^2} + \frac{1}{256R^6}\frac{\epsilon^4}{\pi\rho^2U^2}$.

(8) $-2\int_{S_R}\left(\frac{\partial\varphi^*}{\partial x_1}\frac{\partial\varphi^*}{\partial x_2}\right)n_2\mathrm{d}s = \frac{1}{128}\frac{8R^4-4R^2\epsilon^2-3\epsilon^4+8\sqrt{R^2-\epsilon^2}R^3}{R^6U^2\rho^2\pi}$
$= \frac{1}{16R^2\pi\rho^2U^2} - \frac{1}{32R^4U^2\rho^2\pi}\epsilon^2 - \frac{3}{128R^6U^2\rho^2\pi}\epsilon^4$
$+\frac{1}{16R^3U^2\rho^2\pi}\sqrt{R^2-\epsilon^2}$

(9) $-2\int_{S_R}\left(\frac{\partial\varphi^*}{\partial x_1}\frac{\partial\varphi^*}{\partial x_3}\right)n_3\mathrm{d}s = \frac{1}{16R^2U^2\rho^2\pi} - \frac{1}{32R^4U^2\rho^2\pi}\epsilon^2 - \frac{1}{128R^6U^2\rho^2\pi}\epsilon^4$
$+\frac{1}{16R^3U^2\rho^2\pi}\sqrt{R^2-\epsilon^2}$.

Appendix D: *Evaluation of the axial force over the cylinder* S_C

The following list of results have been obtained by Maple and used in the evaluation:

(1) $\int_{S_C}\left\{(-2UV)\left(-\frac{x_2}{\epsilon}\right)+\left(-2U\frac{\partial\varphi^*}{\partial x_2}\right)\left(-\frac{x_2}{\epsilon}\right)+\left(-2U\frac{\partial\varphi^*}{\partial x_3}\right)\left(-\frac{x_3}{\epsilon}\right)\right\}\mathrm{d}s = 0$ because of antisymmetry of integrand in terms of x_2.

(2) $\int_{S_C}\left(-2V\frac{\partial\varphi^*}{\partial x_1}\right)\left(-\frac{x_2}{\epsilon}\right)\mathrm{d}s = \frac{1}{2}\frac{V}{\rho UR}\sqrt{R^2-\epsilon^2} - \frac{1}{2}\frac{V}{\rho U\sqrt{a^2+\epsilon^2}}a$

(3) $\int_{S_C}\left(-2\frac{\partial\varphi^*}{\partial x_1}\frac{\partial\varphi^*}{\partial x_2}\right)\left(-\frac{x_2}{\epsilon}\right)\mathrm{d}s$

$= \frac{3}{128U^2\rho^2\pi}\frac{\epsilon^6}{R^4(a^2+\epsilon^2)^2} - \frac{1}{32U^2\rho^2\pi}\frac{\epsilon^4}{(a^2+\epsilon^2)^2R^3}\sqrt{R^2-\epsilon^2}$
$+\frac{3}{64U^2\rho^2\pi}\frac{\epsilon^4}{R^4(a^2+\epsilon^2)^2}a^2 - \frac{1}{16U^2\rho^2\pi}\frac{\epsilon^2}{(a^2+\epsilon^2)^2R^3}\sqrt{R^2-\epsilon^2}a^2$
$-\frac{1}{16U^2\rho^2\pi}\frac{\epsilon^2}{(a^2+\epsilon^2)^2R}\sqrt{R^2-\epsilon^2} - \frac{15}{128U^2\rho^2\pi}\frac{\epsilon^2}{(a^2+\epsilon^2)^2} + \frac{3}{128U^2\rho^2\pi}\frac{\epsilon^2}{R^4(a^2+\epsilon^2)^2}a^4$
$+\frac{3}{32U^2\rho^2\pi}\frac{\epsilon^2}{(a^2+\epsilon^2)^{\frac{5}{2}}}a - \frac{1}{32U^2\rho^2\pi(a^2+\epsilon^2)^2R^3}\sqrt{R^2-\epsilon^2}a^4 + \frac{5}{32U^2\rho^2\pi(a^2+\epsilon^2)^{\frac{5}{2}}}a^3$
$-\frac{1}{8U^2\rho^2\pi(a^2+\epsilon^2)^2R}\sqrt{R^2-\epsilon^2}a^2 - \frac{1}{16U^2\rho^2\pi\epsilon^2(a^2+\epsilon^2)^2R}\sqrt{R^2-\epsilon^2}a^4$

$$+\frac{1}{16U^2\rho^2\pi\epsilon^2(a^2+\epsilon^2)^{\frac{5}{2}}}a^5-\frac{1}{8U^2\rho^2\pi\epsilon^2R(a^2+\epsilon^2)}\sqrt{R^2-\epsilon^2}a^2$$
$$-\frac{1}{8U^2\rho^2\pi R(a^2+\epsilon^2)}\sqrt{R^2-\epsilon^2}+\frac{1}{32U^2\rho^2\pi R^3(a^2+\epsilon^2)}\sqrt{R^2-\epsilon^2}a^2$$
$$+\frac{1}{32U^2\rho^2\pi}\frac{\epsilon^2}{R^3(a^2+\epsilon^2)}\sqrt{R^2-\epsilon^2}+\frac{1}{8U^2\rho^2\pi\epsilon^2}\frac{a^3}{(a^2+\epsilon^2)^{\frac{3}{2}}}+\frac{3}{32U^2\rho^2\pi(a^2+\epsilon^2)^{\frac{3}{2}}}a$$
$$+\frac{3}{32U^2\rho^2\pi R^2(a^2+\epsilon^2)^2}a^4+\frac{3}{16U^2\rho^2\pi}\frac{\epsilon^2}{R^2(a^2+\epsilon^2)^2}a^2$$
$$+\frac{3}{32U^2\rho^2\pi}\frac{\epsilon^4}{R^2(a^2+\epsilon^2)^2}-\frac{3}{32U^2\rho^2\pi(a^2+\epsilon^2)^2}a^2.$$

(4) $\int_{S_C}\big(-2\frac{\partial\varphi^*}{\partial x_1}\frac{\partial\varphi^*}{\partial x_3}\big)\big(-\frac{x_3}{\epsilon}\big)\mathrm{d}s$

$$=\frac{1}{128\pi\rho^2U^2}\frac{\epsilon^2}{R^4(a^2+\epsilon^2)^2}a^4+\frac{1}{64\pi\rho^2U^2}\frac{\epsilon^4}{R^4(a^2+\epsilon^2)^2}a^2$$
$$+\frac{1}{128\pi\rho^2U^2}\frac{\epsilon^6}{R^4(a^2+\epsilon^2)^2}+\frac{1}{32\pi\rho^2U^2R^2(a^2+\epsilon^2)^2}a^4$$
$$+\frac{1}{16\pi\rho^2U^2}\frac{\epsilon^2}{R^2(a^2+\epsilon^2)^2}a^2+\frac{1}{32\pi\rho^2U^2}\frac{\epsilon^4}{R^2(a^2+\epsilon^2)^2}-\frac{5}{128\pi\rho^2U^2}\frac{\epsilon^2}{(a^2+\epsilon^2)^2}$$
$$-\frac{1}{32\pi\rho^2U^2(a^2+\epsilon^2)^2}a^2-\frac{1}{16\pi\rho^2U^2\epsilon^2R(a^2+\epsilon^2)}\sqrt{R^2-\epsilon^2}a^2$$
$$-\frac{1}{16\pi\rho^2U^2R(a^2+\epsilon^2)}\sqrt{R^2-\epsilon^2}+\frac{1}{16\pi\rho^2U^2\epsilon^2}\frac{a^3}{(a^2+\epsilon^2)^{\frac{3}{2}}}+\frac{1}{16\pi\rho^2U^2}\frac{a}{(a^2+\epsilon^2)^{\frac{3}{2}}}.$$

Appendix E: *Evaluation of the normal force over the sphere* S_R

The following list of results have been obtained by Maple and used in the evaluation. The spherical coordinate system such that $x_1 = R\cos\theta$, $x_2 = R\sin\theta\cos\phi$ and $x_3 = R\sin\theta\sin\phi$ has been assumed.

(1) $\int_{S_R}\big\{-2\big(\frac{\partial\varphi^*}{\partial x_1}\frac{\partial\varphi^*}{\partial x_2}\big)\big(\frac{x_1}{R}\big)+\big(U^2-V^2+2U\frac{\partial\varphi^*}{\partial x_1}-2V\frac{\partial\varphi^*}{\partial x_2}+\big(\frac{\partial\varphi^*}{\partial x_1}\big)^2-\big(\frac{\partial\varphi^*}{\partial x_2}\big)^2+\big(\frac{\partial\varphi^*}{\partial x_3}\big)^2\big)\big(\frac{x_2}{R}\big)$
$-2\big(V\frac{\partial\varphi^*}{\partial x_3}+\frac{\partial\varphi^*}{\partial x_2}\frac{\partial\varphi^*}{\partial x_3}\big)\big(\frac{x_3}{R}\big)\big\}\mathrm{d}s=0$ because of antisymmetry of integrand in terms of x_2.

(2) $\int_{S_R}(-2UV)\frac{x_1}{R}\mathrm{d}s=\int_{S_R}(-2UV)(\cos\theta)(R^2\sin\theta)\mathrm{d}\phi\mathrm{d}\theta$
$$=\int_{\arccos\left(\frac{\sqrt{R^2-\epsilon^2}}{R}\right)}^{\pi}\Big(\int_0^{2\pi}(-2UV)(\cos\theta)(R^2\sin\theta)\mathrm{d}\phi\Big)\mathrm{d}\theta=2\epsilon^2UV\pi.$$

(3) $\int_{S_R}\big(-2V\frac{\partial\varphi^*}{\partial x_1}\big)\frac{x_1}{R}\mathrm{d}s$
$$=\int_{\arccos\left(\frac{\sqrt{R^2-\epsilon^2}}{R}\right)}^{\pi}\Big(\int_0^{2\pi}\Big(-2V\big(\frac{1}{4\pi\rho UR^2}\sin\theta\cos\phi\big)\Big)(\cos\theta)(R^2\sin\theta)\mathrm{d}\phi\Big)\mathrm{d}\theta=0.$$

Similarly,

(4) $\int_{S_R}\big(-2U\frac{\partial\varphi^*}{\partial x_2}\big)\frac{x_1}{R}\mathrm{d}s=\frac{1}{3\rho}$,

(5) $\int_{S_R}\big(2U\frac{\partial\varphi^*}{\partial x_1}\big)\frac{x_2}{R}\mathrm{d}s=\frac{2}{3\rho}$.

Appendix F: *Evaluation of the side force*

The surface at large R is not symmetric, because of the intersection with the cylindrical surface S_C. In this Appendix section, we show that the contributions from the surface

$(S_C)^\circ$, which is the smaller of the two surfaces formed by the intersection of the surface S_R with S_C in the downstream wake, are all zero.

The following list of results have been obtained by Maple and used in the evaluation:

(1) $\int_{(S_C)^\circ}(U^2+V^2)\frac{x_3}{R}\mathrm{d}s = (U^2+V^2)\int_{(S_C)^\circ}(\sin\phi)\mathrm{d}s = \int_0^{2\pi}\left(\int_\alpha^\beta \epsilon\sin\phi\mathrm{d}x_1\right)\mathrm{d}\phi = 0,$

(2) The integrand of

$$\int_{(S_C)^\circ}\left(-2V\frac{\partial\varphi^*}{\partial x_3}\right)\left(-\frac{x_2}{\epsilon}\right)\mathrm{d}s = \int_0^{2\pi}\int_\alpha^\beta\left(-2V\frac{\partial\varphi^*}{\partial x_3}\right)\left(-\frac{x_2}{\epsilon}\right)\mathrm{d}s \text{ is}$$

$$-\frac{1}{2}V\left(\frac{x_1\epsilon^3(\cos^2\phi\sin\phi)-2\sqrt{\epsilon^2+x_1^2}\epsilon^3(\cos^2\phi\sin\phi)}{\pi\rho U(\sqrt{\epsilon^2+x_1^2}-x_1)^2(\epsilon^2+x_1^2)^{\frac{3}{2}}}\right)$$

$$= \frac{1}{2}V\epsilon^3(\cos^2\phi\sin\phi)\frac{x_1-2\sqrt{\epsilon^2+x_1^2}}{\pi\rho U(\sqrt{\epsilon^2+x_1^2}-x_1)^2(\epsilon^2+x_1^2)^{\frac{3}{2}}}$$

$$= \frac{\left(x_1-2\sqrt{\epsilon^2+x_1^2}\right)(V(\cos^2\phi\sin\phi))}{2\pi\rho U x_1^2(\epsilon^2+x_1^2)^{\frac{3}{2}}}\frac{\epsilon^3}{\left(\sqrt{1+\frac{\epsilon^2}{x_1^2}}-1\right)^2}.$$

Since

$$\sqrt{1+\frac{\epsilon^2}{x_1^2}}-1 = \frac{1}{2}\frac{\epsilon^2}{x_1^2}-\frac{1}{2!2^2}\left(\frac{\epsilon^2}{x_1^2}\right)^2+\frac{1\times3}{3!2^3}\left(\frac{\epsilon^2}{x_1^2}\right)^3-\cdots = O(\epsilon^2),$$

then

$$\frac{\left(x_1-2\sqrt{\epsilon^2+x_1^2}\right)(V(\cos^2\phi\sin\phi))}{2\pi\rho U x_1^2(\epsilon^2+x_1^2)^{\frac{3}{2}}}\frac{\epsilon^3}{\left(\sqrt{1+\frac{\epsilon^2}{x_1^2}}-1\right)^2} = O(\epsilon),$$

and the integral becomes

$$\int_\alpha^\beta\left(-\frac{1}{2}V\frac{x_1\epsilon^3(\cos^2\phi\sin\phi)-2\sqrt{\epsilon^2+x_1^2}\epsilon^3(\cos^2\phi\sin\phi)}{\pi\rho U(\sqrt{\epsilon^2+x_1^2}-x_1)^2(\epsilon^2+x_1^2)^{\frac{3}{2}}}\right)\mathrm{d}x_1 = \left(-\frac{1}{2}V\cos^2\phi\sin\phi\right)$$

$$\frac{-2\sqrt{\epsilon^2+\beta^2}\sqrt{\epsilon^2+\alpha^2}\beta+2\sqrt{\epsilon^2+\beta^2}\sqrt{\epsilon^2+\alpha^2}\alpha-2\sqrt{\epsilon^2+\alpha^2}\beta^2-\sqrt{\epsilon^2+\alpha^2}\epsilon^2+2\sqrt{\epsilon^2+\beta^2}\alpha^2+\sqrt{\epsilon^2+\beta^2}\epsilon^2}{\sqrt{\epsilon^2+\beta^2}\pi\rho U\epsilon\sqrt{\epsilon^2+\alpha^2}},$$

which is zero. For example,

$$\int_{(S_C)^\circ}\left(-2V\frac{\partial\varphi^*}{\partial x_3}\right)\left(-\frac{x_2}{\epsilon}\right)\mathrm{d}s$$

$$= \int_0^{2\pi}\left(\int_\alpha^\beta\left(-\frac{1}{2}V\frac{x_1\epsilon^3(\cos^2\phi\sin\phi)-2\sqrt{\epsilon^2+x_1^2}\epsilon^3(\cos^2\phi\sin\phi)}{\pi\rho U(\sqrt{\epsilon^2+x_1^2}-x_1)^2(\epsilon^2+x_1^2)^{\frac{3}{2}}}\right)\mathrm{d}x_1\right)\mathrm{d}\phi = 0.$$

The evaluation over the surface at large R is therefore equivalent to the evaluation over the surface S_R, which is symmetric.

References

[1] Allen H J and Perkins E W, A study of effects of viscosity on flow over slender inclined bodies of revolution, *Nat. Adv. Comm. Aero.*, Report No. 1048 (1951)

[2] Bruce W C *et al*, Maple V Language Reference Manual, 1st edition (New York: Springer) (1991)

[3] Batchelor G K, Axial flow in trailing line vortices, *J. Fluid Mech.* **20** (1964) 645–658
[4] Batchelor G K, An Introduction to Fluid Dynamics (Cambridge UK: Cambridge University Press) (1967)
[5] Chadwick E and Fishwick N, Lift on slender bodies with elliptical cross section evaluated by using an Oseen flow model, *SIAM J. Appl. Math.* **67** (2007) 1465–1478
[6] Chadwick E and Hatam A, The physical interpretation of the lift discrepancy in Lanchester-Prandtl lifting wing theory for Euler flow, leading to the proposal of an alternative model in Oseen flow, *Proc. R. Soc.* **A463** (2007) 2257–2275
[7] Chadwick E, The far-field Oseen velocity expansion, *Proc. R. Soc.* **A454** (1998) 2059–2082
[8] Chadwick E, A slender-body theory in Oseen flow, *Proc. R. Soc.* **A458** (2002) 2007–2016
[9] Chadwick E, A slender-wing theory in potential flow, *Proc. R. Soc.* **A461** (2005) 415–432
[10] Chadwick E, The vortex line in steady, incompressible Oseen flow, *Proc. R. Soc.* **A462** (2006) 391–401
[11] Euler L, Principia motus fluidorum, presented to the Royal Academy of Prussia (Berlin) (1727)
[12] Fukumoto Y and Moffatt H K, Motion and expansion of a viscous vortex ring, Part 1. A higher-order asymptotic formula for the velocity, *J. Fluid Mech.* **417** (2000) 1–45
[13] Goldstein S, Lectures on Fluid Mechanics (Interscience) (1960)
[14] Katz J and Plotkin A, *Low-Speed Aerodynamics* 2nd edn. (Cambridge, UK: Cambridge University Press) (2001)
[15] Kutta M W, Auftriebskrafte in stromenden Flussigkeiten, *Ill. Aero. Mitt.* **6** (1902) 133
[16] Lagerstrom P A, High Speed Aerodynamics and Jet propulsion, 6th edn. (Princeton, US: Princeton University Press) (1964)
[17] Lamb H, Hydrodynamics, 6th edn. (Cambridge, UK: Cambridge University Press) (1932)
[18] Lighthill M J, An Infomal Introduction to Theoretical Fluid Mechanics (Oxford, UK: Oxford University Press) (1986)
[19] Oseen C W, Neure Methoden Und Ergebnisse In Der Hydrodynamik (Leipzig: Akademische Verlagsgesellschaft) (1927)
[20] Sobolevskii A Eyink G, Moreau R and Frisch U (eds), Euler equations, 250 years on, Aussois, France June 18–23, Guest Edition, *Physica D* (2007)
[21] Stewartson K, On the flow near the trailing-edge of a flat plate, *Mathematika* **16** (1969) 106–121
[22] Stewartson K, On laminar boundary layers near corners, *Q. J. Mech. Appl. Math.* **23** (1970) 137–152
[23] Thwaites B, Incompressible Aerodynamics (Oxford, UK: Oxford University Press) (1960)
[24] Venkatalaxmi A, Sri Padmavati B and Amaranath T, A general solution of Oseen equations, *Fluid Dynamics Res.* (2007)